STUDY ON BEHAVIOR OF CONCRETE FILLED ELLIPTICAL STEEL TUBE MEMBERS PART II : UNDER BENDING AND ECCENTRIC COMPRESSION

Xiaoxiong Zha [1,*], Guobin Gong [2] and Xichao Liu [2]

[1] *Shenzhen Graduate School, Harbin Institute of Technology, Shenzhen 518055, China*
[2] *Shenzhen Graduate School, Harbin Institute of Technology, Shenzhen 518055, China*
**(Corresponding author: E-mail: zhaxx@hit.edu.cn)*

Received: 28 April 2011; Revised: 17 February 2012; Accepted: 29 February 2012

ABSTRACT: In this paper, based on the ideology of "unified theory", the theoretical calculation equations of ultimate flexural capacity for concrete filled elliptical steel tube members (CFEST) around long and short axes are derived and compared with and verified by finite element simulations. Modified equations are then proposed for practical applications on the basis of the flexural capacity for circular concrete filled steel tube members. Under the guidance of "unified theory" and parametric analysis, the simplified practical calculation equations of capacity for CFEST members under eccentric compression are obtained, and mechanical behavior of a series of CFEST members with different section dimensions is conducted using finite element analysis.

Keywords: Elliptical concrete filled steel tube, Unified theory, Bending, Eccentric compression, Finite element, Parametric analysis

1. INTRODUCTION

In the framework of "unified theory" proposed by Zhong [1], the concrete filled steel tube (CFST) can be considered to be one unified material, on which the unified capacity is based rather than the simple superposition of capacity of concrete and steel tube. In other words, the unified compressive strength can be expressed by one parameter f_{sc}^{y}, which incorporates the effect of the concrete-steel interaction. According to ultimate balance theory, the ultimate flexural bending capacity is derived for CFEST members around strong and weak axes. Then the theory is modified and amended with the help of finite element simulation results, and simplified equations are obtained for ultimate flexural bending capacity for CFEST members. Based on the existing interaction equation of $N/N_0 \sim M/M_0$ for flexural capacity for concrete filled circular steel tube, a series of flexural members are analyzed by using finite element simulations for different elliptical aspect ratios. And interaction equations of $N/N_0 \sim M/M_0$ are obtained for the CFEST members.

2. FINITE ELEMENT SIMULATION OF CFEST FOR COMPRESSIVE AND FLEXURAL MEMBERS

A general-purpose finite element software ABAQUS is used for simulating CFEST members. Solid elements are used for both steel tube and concrete, and the nodes are tied together, i.e. no sliding. The concrete damaged plasticity model is employed for concrete material. The concrete axial compressive stress-strain relation is shown in Figure 1, and the mathematical equation of expression can be described as follows. More details can be found in GB50010 [2]

when $\varepsilon \le \varepsilon_e$, $\sigma = E_c\varepsilon$, $E_c = 0.3 f_{ck}/\varepsilon_e$;

when $\varepsilon_e \le \varepsilon \le \varepsilon_c$, $\sigma = f_{ck}\left[\alpha_a\left(\frac{\varepsilon}{\varepsilon_c}\right)+(3-2\alpha_a)\left(\frac{\varepsilon}{\varepsilon_c}\right)^2+(\alpha_a-2)\left(\frac{\varepsilon}{\varepsilon_c}\right)^3\right]$;

when $\varepsilon_c \le \varepsilon \le \varepsilon_u, \sigma = f_{ck} \dfrac{\varepsilon/\varepsilon_c}{\alpha_d(\varepsilon/\varepsilon_c - 1)^2 + \varepsilon/\varepsilon_c}$;

where:

ε_e —compressive strain corresponding to stress with the value of $0.3 f_{ck}$ at hardening stage

ε_c —compressive strain corresponding to stress with the peak value of f_{ck}

ε_c —compressive strain corresponding to stress with the value of $0.5 f_{ck}$ at softening stage

α_a , α_d —model constants

The axial tensile stress-strain relationship is based on energy criterion of concrete, i.e. softened stress-fracture energy relation and the stress-strain curve is shown in Figure 2, with the mathematical equation of expression described as follows. G_f and σ_{t0} are concrete fracture energy (the energy required to cause one continuous crack per unit area), and failure stress respectively. When $f_{ck} = 20\text{MPa}, G_f = 40\text{N/m}$; when $f_{ck} = 40\text{MPa}, G_f = 120\text{N/m}$, and the values of G_f can be obtained using linear interpolation corresponding to other values of f_{ck}.

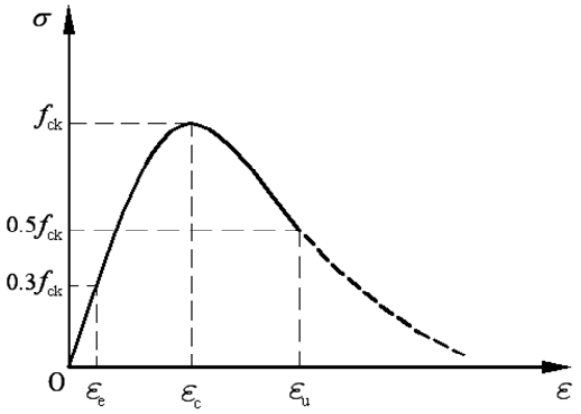

Figure 1. Concrete Compressive Stress-strain Relation of concrete

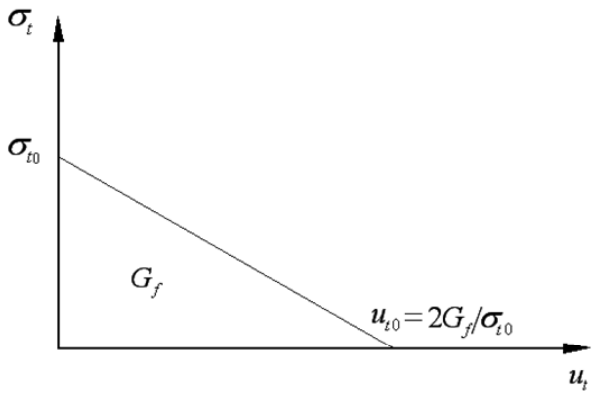

Figure 2. Concrete Tensile Softening Model of concrete

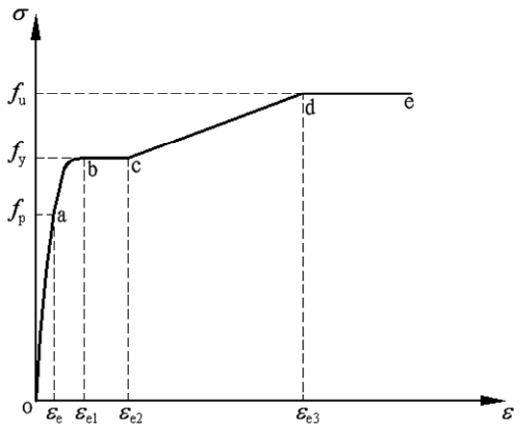

Figure 3. Steel Stress-strain Relation of steel

Axial stress-strain relation of steel is shown in Figure 3, and the mathematical expression can be described as follows：

$$\sigma_s = \begin{cases} E_s\varepsilon_s & \varepsilon_s \le \varepsilon_e \\ -A\varepsilon_s^2 + B\varepsilon_s + C & \varepsilon_e \le \varepsilon_s \le \varepsilon_{e1} \\ f_y & \varepsilon_{e1} \le \varepsilon_s \le \varepsilon_{e2} \\ f_y\left[1+0.6\dfrac{\varepsilon_s-\varepsilon_{e2}}{\varepsilon_{e3}-\varepsilon_{e2}}\right] & \varepsilon_{e2} \le \varepsilon_s \le \varepsilon_{e3} \\ 1.6f_y & \varepsilon_s > \varepsilon_{e3} \end{cases}$$

where,

f_p is proportional limit value of steel

f_y is yield strength value of steel

f_u is ultimate strength value of steel

$\varepsilon_e = 0.8f_y / E_s$, $\varepsilon_{e1} = 1.5\varepsilon_e$, $\varepsilon_{e2} = 10\varepsilon_{e1}$, $\varepsilon_{e3} = 100\varepsilon_{e1}$, $B = 2A\varepsilon_{e1}$,

$A = 0.2f_y / (\varepsilon_{e1} - \varepsilon_e)^2$, $C = 0.8f_y + A\varepsilon_e^{\,2} - B\varepsilon_e$.

and the details can be found in Han [3].

Figure 4 shows an established CFEST finite element model with solid elements for steel and concrete and there are three layers of meshed elements along the steel tube thickness direction.

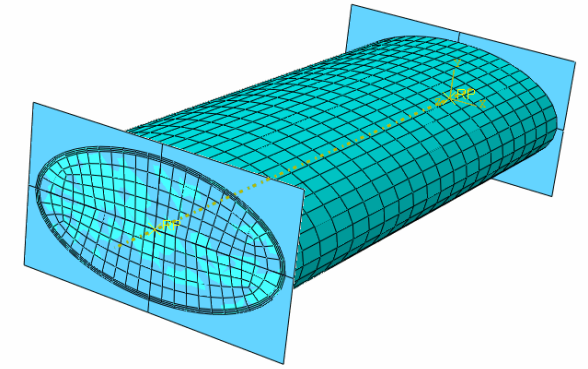

Figure 4. Finite Element Model for CFEST

In order to verify the accuracy of the finite element model, concrete filled steel circular tube for eccentric compression is simulated using finite element in Chen et al. [4] and Yu and Ding [5], and the simulation results agree well with the test results, see Liu [6].

3. THE FLEXURAL BEHAVIOR AROUND THE LONG/WEAK AXIS OF CONCRETE FILLED ELLIPTICAL STEEL TUBE

3.1 Theoretical Equation Derivation of Flexural Bending Capacity around Long Axis

All the derivations in this paper are limited to uniaxial bending only. The stress distribution of CFEST at limit state, and the cross section dimensions are shown in Figure 5.

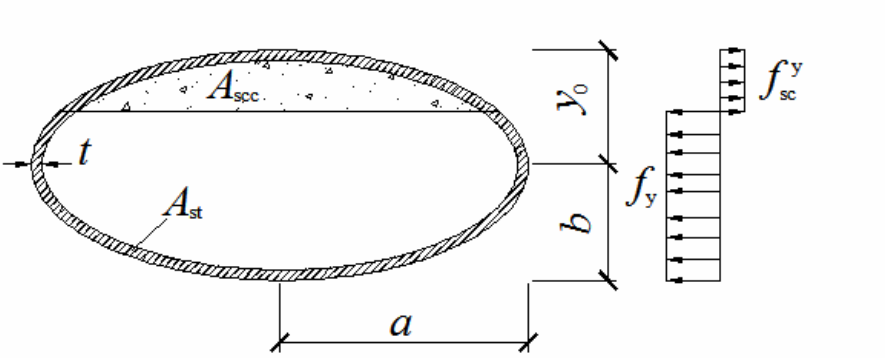

Figure 5. Stress Distribution Bent Around Long Axis for CFEST at Limit State and Section Dimensions

When the member is at limit state, the section stress distribution is as shown in Figure 5. According to static equilibrium, the location of neutral axis can be determined, i.e. y0 (distance of the section centroid to neutral axis).

. $\sum N = 0 \Rightarrow$

$$A_{st} f_y - A_{scc} f_{sc}^{y} = 0 \tag{1}$$

$$A_{st} = \pi ab - \pi(a-t)(b-t) - 2ab\left[\frac{\pi}{4} - \frac{1}{2}\arcsin\left(\frac{y_0}{b}\right) - \frac{y_0}{2b}\sqrt{1-\left(\frac{y_0}{b}\right)^2}\right] + 2(a-t)(b-t)\left[\frac{\pi}{4} - \frac{1}{2}\arcsin\left(\frac{y_0}{(b-t)}\right) - \frac{y_0}{2(b-t)}\sqrt{1-\left(\frac{y_0}{(b-t)}\right)^2}\right] \tag{2}$$

$$A_{scc} = 2ab\left[\frac{\pi}{4} - \frac{1}{2}\arcsin\left(\frac{y_0}{b}\right) - \frac{y_0}{2b}\sqrt{1-\left(\frac{y_0}{b}\right)^2}\right] \tag{3}$$

where A_{st} —section area for steel tube in tension zone;
A_{scc} —combined section area in compression zone
a —half length of long axis for elliptical section
b —half length of short axis for elliptical section
t —steel tube thickness
y_0 — distance of the section centroid to neutral axis.
f_y —yield strength of steel

f_{sc}^{y}—combined characteristic strength for concrete filled steel tube

According to the location of neutral axis based on Eq. 1, the limit bending moment capacity can be obtained by taking moment about the neutral axis contributed by tensile stress and compressive stress：

$$M_0 = M_s + M_{sc} \tag{4}$$

$$\begin{aligned} M_s = 2 f_y \Bigg\{ & \left[\frac{\pi}{4} a b y_0 + \frac{1}{2} a b y_0 \arcsin\left(\frac{y_0}{b}\right) + \frac{1}{3} a b^2 \sqrt{1-\left(\frac{y_0}{b}\right)^2} \right. \\ & \left. + \frac{1}{6} a y_0^2 \sqrt{1-\left(\frac{y_0}{b}\right)^2} \right] - \left[\frac{\pi}{4}(a-t)(b-t) y_0 + \frac{1}{2}(a-t)(b-t) y_0 \arcsin\left(\frac{y_0}{b-t}\right) \right. \\ & \left. + \frac{1}{3}(a-t)(b-t)^2 \sqrt{1-\left(\frac{y_0}{b-t}\right)^2} + \frac{1}{6}(a-t) y_0^2 \sqrt{1-\left(\frac{y_0}{b-t}\right)^2} \right] \Bigg\} \end{aligned} \tag{5}$$

$$M_{sc} = 2 f_{sc}^{y} \left\{ \frac{1}{3} a b^2 \left[1-\left(\frac{y_0}{b}\right)^2 \right]^{\frac{3}{2}} - a b y_0 \left[\frac{\pi}{4} - \frac{1}{2}\left(\frac{y_0}{b}\right) \sqrt{1-\left(\frac{y_0}{b}\right)^2} - \frac{1}{2} \arcsin\left(\frac{y_0}{b}\right) \right] \right\} \tag{6}$$

As the tension strength of concrete is ignored in the above derivation, the actual limit bending capacity will be larger than calculated by Eq. 4. By comparison with finite element analysis results, the bending capacity of CFEST can be approximately expressed as follows:

$$M = 1.2 M_0 \tag{7}$$

From Eqs. 4, 5, 6, we know that the factors affecting the limit flexural capacity for CFEST are mainly steel strength, concrete compressive strength and member section shape. In order to verify the applicability of the theoretical Eq. 5 to 7, a total of 77 finite element models are established and the results are compared with those from the equations, with an average of 1.004 and variance of 0.0008 , see Liu [6].

3.2 Practical Equation of Flexural Bending Capacity around Long Axis

Comparison of theoretical results and finite element simulation results indicates that the limit state equilibrium based limit state flexural capacity for concrete filled steel tube can be reasonably used to calculate the limit flexural capacity. However, the solution procedures are quite complex and not applicable to practical engineering. With finite element analysis results, an equation of flexural bending capacity around long axis for practical purpose is obtained as follows:

$$M = \gamma_m W_{sc} f_{sc}^{y} \tag{8}$$

$$\gamma_m = -0.4832 k\xi + 1.9264 (k\xi)^{0.5} \tag{9}$$

where

γ_m is cross section plastic development coefficient

W_{sc} is modulus of the combined section

k is confining adjustment factor，when around long axis，

$$k = (a/b)^{0.12}$$

The comparison of finite element simulation results and Eq. 8 shows that an average of 1.017 and variance of 0.004, see Appendix 2 and also Liu [6]. Compared with Eq. 7, Eq. 8 gives a relatively little larger value, but the equation form is simplified, which is more suitable for practical engineering.

4. THE FLEXURAL BEHAVIOR AROUND THE SHORT/STRONG AXIS OF CFEST [7-9]

4.1 Theoretical Derivation of Flexural Bending Capacity around Short Axis

The stress distribution of CFEST at limit state, and the cross section dimensions are shown in Figure 5. y_0 is the distance of the section centroid to neutral axis.

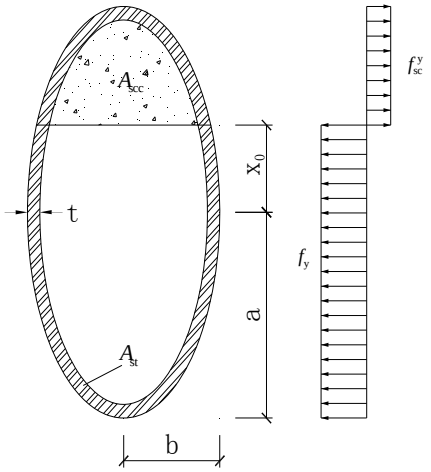

Figure 6. Stress Distribution Bent around Short Axis for CFEST at Limit State and Section Dimensions

When the member is at limit state, the section stress distribution is as shown in Figure 6. According to static equilibrium, the location of neutral axis can be determined, i.e. x_0 . $\sum N = 0$ =>

$$A_{st} f_y - A_{scc} f_{sc}^y = 0 \tag{10}$$

$$\begin{aligned} A_{st} = {} & \pi ab - \pi(a-t)(b-t) - 2ab\left[\frac{\pi}{4} - \frac{1}{2}\arcsin\left(\frac{x_0}{a}\right) - \frac{x_0}{2a}\sqrt{1-\left(\frac{x_0}{a}\right)^2}\right] \\ & +2(a-t)(b-t)\left[\frac{\pi}{4} - \frac{1}{2}\arcsin\left(\frac{x_0}{(a-t)}\right) - \frac{x_0}{2(a-t)}\sqrt{1-\left(\frac{x_0}{(a-t)}\right)^2}\right] \end{aligned} \tag{11}$$

$$A_{\mathrm{scc}} = 2ab\left[\frac{\pi}{4} - \frac{1}{2}\arcsin\left(\frac{x_0}{a}\right) - \frac{x_0}{2a}\sqrt{1-\left(\frac{x_0}{a}\right)^2}\right] \tag{12}$$

According to the location of neutral axis based on Eq. 10, the limit bending moment capacity can be obtained by taking moment about the neutral axis contributed by tensile stress and compressive stress：

$$M_0 = M_{\mathrm{s}} + M_{\mathrm{sc}} \tag{13}$$

$$\begin{aligned} M_{\mathrm{s}} = 2f_{\mathrm{y}}\Bigg\{&\left[\frac{\pi}{4}abx_0 + \frac{1}{2}abx_0\arcsin\left(\frac{x_0}{a}\right) + \frac{1}{3}ba^2\sqrt{1-\left(\frac{x_0}{a}\right)^2}\right.\\ &\left.+\frac{1}{6}bx_0^2\sqrt{1-\left(\frac{x_0}{a}\right)^2}\right] - \left[\frac{\pi}{4}(a-t)(b-t)x_0 + \frac{1}{2}(a-t)(b-t)x_0\arcsin\left(\frac{x_0}{a-t}\right)\right.\\ &\left.+\frac{1}{3}(b-t)(a-t)^2\sqrt{1-\left(\frac{x_0}{a-t}\right)^2} + \frac{1}{6}(b-t)x_0^2\sqrt{1-\left(\frac{x_0}{a-t}\right)^2}\right]\Bigg\} \end{aligned} \tag{14}$$

$$M_{\mathrm{sc}} = 2f_{\mathrm{sc}}^{\mathrm{y}}\left\{\frac{1}{3}ba^2\left[1-\left(\frac{x_0}{a}\right)^2\right]^{\frac{3}{2}} - abx_0\left[\frac{\pi}{4} - \frac{1}{2}\left(\frac{x_0}{a}\right)\sqrt{1-\left(\frac{x_0}{a}\right)^2} - \frac{1}{2}\arcsin\left(\frac{x_0}{a}\right)\right]\right\} \tag{15}$$

By finite element analysis, the bending capacity of CFEST can be approximately expressed as follows:

$$M = 1.17M_0 \tag{16}$$

The theoretical results are compared with those from finite element simulations, with an average of 1.003 and variance of 0.0003, see Liu [6].

4.2 Practical Flexural Bending Capacity around Short Axis

Comparison of theoretical results and finite element simulation results indicates that the limit state equilibrium based limit state flexural capacity for concrete filled steel tube can reasonably used to calculate the limit flexural capacity. However, the solution procedures are quite complex and not applicable to practical engineering. With finite element analysis results, an equation of flexural bending capacity around long axis for practical purpose is obtained as follows:

$$M = \gamma_{\mathrm{m}} W_{\mathrm{sc}} f_{\mathrm{sc}}^{\mathrm{y}} \tag{17}$$

$$\gamma_{\mathrm{m}} = -0.4832k\xi + 1.9264\left(k\xi\right)^{0.5} \tag{18}$$

where

γ_m is cross section plastic development coefficient

W_{sc} is modulus of the combined section

k is confining adjustment factor， when around short axis，

$k = (b/a)^{0.6}$.

The comparison of finite element simulation results and Eq. 17 shows that an average of 0.993 and variance of 0.006, see Appendix 3 and also Liu [6]. Compared with Eq. 16, Eq. 17 gives a relatively little smaller value, but the equation form is simplified, which is more suitable for practical engineering.

5. INTERACTION EQUATIONS OF ECCENTRIC COMPRESSION CAPACITY FOR CFEST MEMBERS [9-11]

The actions of compression and bending moment on compressive and flexural member may be caused by different loads, i.e. pressure and bending moment can be two independent variables. For the one-way compressive flexural/bending structures, there are mainly three different loading paths, as shown in Figure 7 [3].

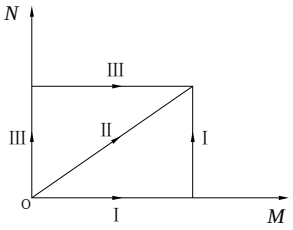

Figure 7. Loading Paths for Compressive and Flexural Member

In this paper, loading path Ⅱ is adopted for finite element simulation of concrete filled elliptical steel tube, and the main concern is to analyze the concrete filled elliptical steel tube behavior with different cross sections and under different eccentricities.

5.1 Interaction Equations of Eccentric Compression Capacity around Long Axis for CFEST Members

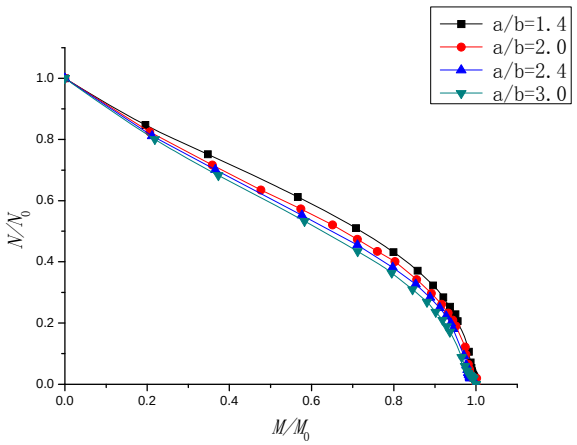

Figure 8. $N/N_0 \sim M/M_0$ of Eccentric Compression Capacity around Long Axis for Concrete Filled Elliptical Steel Tube

In this paper, finite element analysis is used for obtaining the $N/N_0 \sim M/M_0$ interaction curves. In Figure 8, there are balanced points in the curve of $N/N_0 \sim M/M_0$, which moves down as the increase of steel ratio. Considering that limited value range for the steel ratio, the balanced points are different curves are unified to one point $N/N_0 = 0.2$ [2]. The interaction curve is divided to two segments. Curve fitting is used for obtaining the equation. Considering safety factors, modification factor is introduced and the final interaction equations of eccentric compression capacity around long axis for CFEST is as follows

1) when $\frac{N}{\varphi A_{sc}} \geq 0.2 f_{sc}^{y}$

$$\frac{N}{N_0} + \frac{\beta_m M}{1.32(1-0.4N/N_E)M_0} \leq 1 \tag{19}$$

2) when $\frac{N}{\varphi A_{sc}} < 0.2 f_{sc}^{y}$

$$-\frac{N}{7N_0} + \frac{\beta_m M}{(1-0.4N/N_E)M_0} \leq 1 \tag{20}$$

5.2 Interaction Equations of Eccentric Compression Capacity around Short Axis for CFEST Members

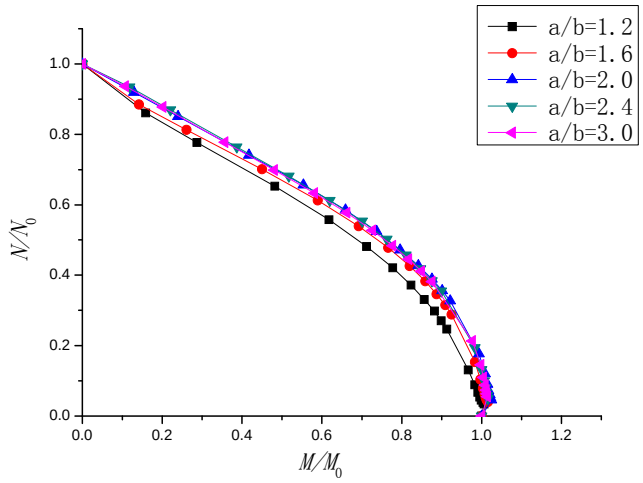

Figure 9. $N/N_0 \sim M/M_0$ of Eccentric Compression Capacity around Short Axis for Concrete Filled Elliptical Steel Tube

Finite element analysis is used for obtaining the $N/N_0 \sim M/M_0$ interaction curves as shown in Figure 9. Curve fitting is used for obtaining the equation. Considering safety factors, modification factor is introduced and the final interaction equations of eccentric compression capacity around short axis for CFEST is as follows

1) when $\frac{N}{\varphi A_{sc}} \geq 0.2 f_{sc}^{y}$

$$\frac{N}{N_0} + \frac{\beta_m M}{1.45(1-0.4N/N_E)M_0} \leq 1 \tag{21}$$

2) when $\frac{N}{\varphi A_{sc}} < 0.2 f_{sc}^{y}$

$$-\frac{N}{7N_0}+\frac{\beta_m M}{(1-0.4N/N_E)M_0}\le 1 \tag{22}$$

6. CONCLUDING REMARKS

In this paper the limit equilibrium method is used to derive theoretical bending capacity equation for elliptical concrete filled steel tube members under uniaxial bending, and the equation based results are compared with and verified by the finite element simulation results. In view of complexity in the theoretical equations, modifications are made and simplified and practical equations are obtained which are suitable for practical engineering and also verified by finite element simulation analysis.

For eccentric compression members of concrete filled steel tubes, a series of elliptical cross section, around long and short axis eccentric compression models are established based on finite element analysis. The interaction curves $N/N_0 \sim M/M_0$ are obtained by finite element simulations. Finally, according to the $N/N_0 \sim M/M_0$ curves for different elliptical section dimensions and for different eccentricities around long and short axes, equations are obtained which can be applied to practical engineering.

REFERENCES

[1] Zhong, S T., “Unified Theory of Concrete Filled Steel Tube - Theoretical Research and Application”, Tsinghua University Press, 2006 (in Chinese)

[2] GB50010-2002, Code for Design of Concrete Structures. Ministry of Construction, People’s Republic of China. (in Chinese)

[3] Han, L.H., “Concrete Filled Steel Tube Structure - Theory and Practice”, Science Press. 2004 (in Chinese)

[4] Chen, B.C., Ou, Z.Q., Wang, L.Y. and Han, L.H., “Eccentric Bearing Capacity Analysis of Concrete Filled Steel Tube”, 2002, Vol. 30, No. 6, pp. 838-844 (in Chinese).

[5] Yu, Z.W. and Ding, X.F., “Mechanical Properties of Concrete Filled Circular Steel Tube Eccentric Loaded Columns”, 2008, Vol. 21, No. 1, pp. 40-46 (in Chinese).

[6] Liu, X.C., “Study of Basic Properties of Concrete Filled Elliptical Steel Tube”, Master Thesis, Harbin Institute of Technology Shenzhen Graduate School, 2010, Vol. 6 (in Chinese).

[7] Yang, H., Lam, D. and Gardner, L., “Testing and Analysis of Concrete-filled Elliptical Hollow Sections”, Engineering Structures, 2008, Vol. 30, No. 2, pp. 3771-3781.

[8] Eiichi Inai, Akiyoshi Mukai, Makoto Kai, Hiroyoshi Tokinoya, Toshiyuki Fukumoto, Koji Mori6, “Behavior of Concrete-Filled Steel Tube Beam Columns”, ASCE, Journal of Structural Engineering, 2004, Vol. 130, No. 2, pp. 189-202.

[9] Chan, T.M. and Gardner, L., “Flexural Buckling of Elliptical Hollow Section Columns”, ASCE, Journal of Structural Engineering, 2009, Vol. 135, No. 5, pp. 546-557.

[10] Amit, H., Varma, James M., Ricles, Richard Sause, Lu, L.W., “Experimental Behavior of High Strength Square Concrete-Filled Steel Tube Beam-Columns”, ASCE, Journal of Structural Engineering, 2002, Vol. 128, No. 3, pp. 309-318.

[11] Toshiaki Fujimoto, Akiyoshi Mukai, Isao Nishiyama, Kenji Sakino, “Behavior of Eccentrically Loaded Concrete-Filled Steel Tubular Columns”, ASCE, Journal of Structural Engineering, 2004, Vol. 130, No. 2, pp. 203-212.

Appendix 1: Notations

ε_e : compressive strain corresponding to stress with the value of $0.3f_{ck}$ at hardening stage

ε_c : compressive strain corresponding to stress with the peak value of f_{ck} or $0.5f_{ck}$ at softening stage

α_a , α_d : model constants

f_p : proportional limit value of steel

f_y : yield strength value of steel

f_u : ultimate strength value of steel

A_{st} : section area for steel tube in tension zone

A_{scc} : combined section area in compression zone

a : half length of long axis for elliptical section

b : half length of short axis for elliptical section

t : steel tube thickness

y_0 : distance of the section centroid to neutral axis.

f_{sc}^{y} : combined characteristic strength for concrete filled steel tube

γ_m : cross section plastic development coefficient

W_{sc} : section modulus of the combined section

k : confining adjustment factor

Appendix 2: Comparison of Finite Element Analysis and Theoretical Equation for Flexural Capacity for CFEST Members Bent around Long Axis

$2a$ (mm)	$2b$ (mm)	t (mm)	f_{ck} (N/mm^2)	f_y (N/mm^2)	M_c (kN×m)	M_{FEM} (kN×m)	$\frac{M_c}{M_{FEM}}$
151.79	94.87	2.91	20.1	235	14.86	15.06	0.987
161.00	89.44	2.87	20.1	235	15.20	15.80	0.962
169.71	84.85	2.82	20.1	235	15.52	16.46	0.943
151.79	94.87	2.91	26.8	235	15.55	15.70	0.990
161.00	89.44	2.87	26.8	235	15.89	16.50	0.963
169.71	84.85	2.82	26.8	235	16.20	17.22	0.941
151.79	94.87	2.91	20.1	345	21.34	20.92	1.020
161.00	89.44	2.87	20.1	345	21.91	21.90	1.000
151.79	94.87	2.91	32.4	235	16.16	16.19	0.998
161.00	89.44	2.87	32.4	235	16.51	17.04	0.969
169.71	84.85	2.82	20.1	345	22.44	22.78	0.985
177.99	80.90	2.77	20.1	345	22.92	23.82	0.962
185.90	77.46	2.72	20.1	345	23.37	24.78	0.943
151.79	94.87	2.91	20.1	390	24.12	23.25	1.037
161.00	89.44	2.87	20.1	390	24.81	24.33	1.020
169.71	84.85	2.82	20.1	390	25.45	25.28	1.006
177.99	80.90	2.77	20.1	390	26.03	26.43	0.985
185.90	77.46	2.72	20.1	390	26.58	27.49	0.967
193.49	74.42	2.67	20.1	390	27.09	28.41	0.954
200.80	71.71	2.63	20.1	390	27.58	29.16	0.946
207.85	69.28	2.58	20.1	390	28.04	30.27	0.926

141.99	101.42	3.94	20.1	345	26.74	25.02	1.069
151.79	94.87	3.88	20.1	345	27.74	26.41	1.050
161.00	89.44	3.82	20.1	345	28.64	27.70	1.034
169.71	84.85	3.76	20.1	345	29.46	28.92	1.019
177.99	80.90	3.69	20.1	345	30.22	30.02	1.007
185.90	77.46	3.62	20.1	345	30.94	31.20	0.992
193.49	74.42	3.56	20.1	345	31.61	32.12	0.984
200.80	71.71	3.50	20.1	345	32.25	33.19	0.972
207.85	69.28	3.43	20.1	345	32.86	34.30	0.958
151.79	94.87	4.85	20.1	345	33.79	31.66	1.067
161.00	89.44	4.77	20.1	345	35.08	33.16	1.058
169.71	84.85	4.69	20.1	345	36.26	34.73	1.044
177.99	80.90	4.61	20.1	345	37.37	36.05	1.037
185.90	77.46	4.52	20.1	345	38.40	37.35	1.028
193.49	74.42	4.44	20.1	345	39.38	38.65	1.019
200.80	71.71	4.36	20.1	345	40.32	39.90	1.011
207.85	69.28	4.28	20.1	345	41.22	41.11	1.003

Appendix 3: Comparison of Finite Element Analysis and Theoretical Equation for Flexural Capacity for CFEST Members Bent around Short Axis

$2a$ (mm)	$2b$ (mm)	t (mm)	f_{ck} (N/mm^2)	f_y (N/mm^2)	x_0 (mm)	M_c (kN×m)	M_{FEM} (kN×m)	$\frac{M_c}{M_{FEM}}$
131.45	109.54	2.99	20.1	235	22.64	11.57	13.19	1.004
169.71	84.85	2.82	20.1	235	26.42	9.09	16.46	0.993
200.80	71.71	2.63	20.1	235	29.28	7.76	19.08	0.987
207.85	69.28	2.58	20.1	235	29.99	7.50	19.81	0.977
131.45	109.54	2.99	26.8	235	26.05	11.96	13.71	1.001
141.99	101.42	2.96	26.8	235	27.42	11.13	14.69	0.998
151.79	94.87	2.91	26.8	235	28.77	10.42	15.70	0.986
161.00	89.44	2.87	26.8	235	29.88	9.87	16.50	0.987
169.71	84.85	2.82	26.8	235	30.98	9.39	17.22	0.989
177.99	80.90	2.77	26.8	235	32.01	8.97	18.07	0.981
185.90	77.46	2.72	26.8	235	32.99	8.60	18.84	0.976
193.49	74.42	2.67	26.8	235	33.94	8.27	19.50	0.975
200.80	71.71	2.63	26.8	235	34.74	8.00	20.05	0.980
207.85	69.28	2.58	26.8	235	35.64	7.73	20.84	0.970
207.85	69.28	2.58	32.4	235	39.70	7.89	21.64	0.963
131.45	109.54	2.99	20.1	345	19.03	16.39	18.42	1.017
141.99	101.42	2.96	20.1	345	19.78	15.26	19.65	1.014
185.90	77.46	2.72	20.1	345	22.92	11.84	24.78	1.000
193.49	74.42	2.67	20.1	345	23.48	11.40	25.61	1.000
185.90	77.46	2.72	20.1	390	21.72	13.28	27.49	1.008
193.49	74.42	2.67	20.1	390	22.25	12.79	28.41	1.008
200.80	71.71	2.63	20.1	390	22.52	12.36	29.16	1.014
207.85	69.28	2.58	20.1	390	23.20	11.96	30.27	1.005
131.45	109.54	3.98	20.1	345	16.32	20.96	23.37	1.024
141.99	101.42	3.94	20.1	345	16.89	19.53	25.02	1.018
185.90	77.46	3.62	20.1	345	19.41	15.20	31.20	1.015

193.49	74.42	3.56	20.1	345	19.82	14.66	32.12	1.020
200.80	71.71	3.50	20.1	345	20.24	14.17	33.19	1.019
151.79	94.87	4.85	20.1	345	15.23	22.19	31.66	1.024
161.00	89.44	4.77	20.1	345	15.69	21.02	33.16	1.026
169.71	84.85	4.69	20.1	345	16.10	20.04	34.73	1.023
177.99	80.90	4.61	20.1	345	16.49	19.19	36.05	1.026
185.90	77.46	4.52	20.1	345	16.97	18.42	37.35	1.026
193.49	74.42	4.44	20.1	345	17.39	17.76	38.65	1.026
200.80	71.71	4.36	20.1	345	17.82	17.16	39.90	1.026
207.85	69.28	4.28	20.1	345	18.28	16.62	41.11	1.025

Appendix 4: Comparison of Finite Element Analysis and Theoretical Equation for CFEST Members under Eccentric Compression around Long Axis

$2a$ (mm)	$2b$ (mm)	t (mm)	L (mm)	λ	e_0 (mm)	N (kN)	M (kN×m)	Interaction equation
141.99	101.42	2.96	1000	39.44	5	411.66	2.06	1.001
141.99	101.42	2.96	1000	39.44	10	365.14	3.65	1.023
141.99	101.42	2.96	1000	39.44	50	180.26	9.01	1.031
141.99	101.42	2.96	1000	39.44	60	156.85	9.41	1.010
141.99	101.42	2.96	1000	39.44	70	138.14	9.67	0.990
141.99	101.42	2.96	1000	39.44	80	122.98	9.84	0.970
141.99	101.42	2.96	1000	39.44	90	110.90	9.98	0.955
141.99	101.42	2.96	1000	39.44	200	51.62	10.32	0.972
141.99	101.42	2.96	1000	39.44	300	34.57	10.37	0.980
141.99	101.42	2.96	1000	39.44	400	25.97	10.39	0.983
141.99	101.42	2.96	1000	39.44	500	20.81	10.40	0.986
141.99	101.42	2.96	1000	39.44	600	17.37	10.42	0.988
141.99	101.42	2.96	1000	39.44	700	14.91	10.43	0.990
141.99	101.42	2.96	1000	39.44	800	13.06	10.45	0.992
141.99	101.42	2.96	1000	39.44	900	11.62	10.46	0.993
141.99	101.42	2.96	1000	39.44	1000	10.47	10.47	0.994
169.71	84.85	2.82	1000	47.14	5	375.22	1.88	0.988
169.71	84.85	2.82	1000	47.14	10	325.95	3.26	0.999
169.71	84.85	2.82	1000	47.14	15	288.90	4.33	1.009
169.71	84.85	2.82	1000	47.14	20	260.83	5.22	1.022
169.71	84.85	2.82	1000	47.14	25	236.73	5.92	1.028
207.85	69.28	2.58	1000	57.74	900	8.63	7.77	0.991
207.85	69.28	2.58	1000	57.74	1000	7.79	7.79	0.993
169.71	84.85	2.82	1000	47.14	30	215.50	6.47	1.026
169.71	84.85	2.82	1000	47.14	35	197.42	6.91	1.023
169.71	84.85	2.82	1000	47.14	40	182.42	7.30	1.022
169.71	84.85	2.82	1000	47.14	50	155.60	7.78	1.002
169.71	84.85	2.82	1000	47.14	500	17.91	8.95	0.981
169.71	84.85	2.82	1000	47.14	600	14.94	8.97	0.983
169.71	84.85	2.82	1000	47.14	700	12.82	8.97	0.984
169.71	84.85	2.82	1000	47.14	800	11.22	8.98	0.985
169.71	84.85	2.82	1000	47.14	900	9.98	8.99	0.986
169.71	84.85	2.82	1000	47.14	1000	9.02	9.10	1.000

185.90	77.46	2.72	1000	51.64	5	394.42	1.80	0.981
185.90	77.46	2.72	1000	51.64	10	340.65	3.11	0.992
185.90	77.46	2.72	1000	51.64	20	268.37	4.90	1.006
185.90	77.46	2.72	1000	51.64	30	220.76	6.04	1.010
185.90	77.46	2.72	1000	51.64	40	185.50	6.77	1.002
185.90	77.46	2.72	1000	51.64	50	158.89	7.25	0.988
185.90	77.46	2.72	1000	51.64	60	137.81	7.54	0.970
185.90	77.46	2.72	1000	51.64	70	121.21	7.74	0.952
185.90	77.46	2.72	1000	51.64	200	45.17	8.24	0.963
185.90	77.46	2.72	1000	51.64	300	30.30	8.30	0.972
185.90	77.46	2.72	1000	51.64	400	22.79	8.32	0.976
185.90	77.46	2.72	1000	51.64	500	18.27	8.33	0.978
185.90	77.46	2.72	1000	51.64	600	15.25	8.35	0.980
185.90	77.46	2.72	1000	51.64	700	13.10	8.37	0.983
185.90	77.46	2.72	1000	51.64	800	11.46	8.36	0.983
185.90	77.46	2.72	1000	51.64	900	10.19	8.37	0.984
185.90	77.46	2.72	1000	51.64	1000	9.18	8.38	0.984
207.85	69.28	2.58	1000	57.74	5	342.73	1.71	0.977
207.85	69.28	2.58	1000	57.74	10	292.18	2.92	0.980
207.85	69.28	2.58	1000	57.74	20	228.25	4.57	0.993
207.85	69.28	2.58	1000	57.74	30	185.83	5.57	0.991
207.85	69.28	2.58	1000	57.74	40	155.62	6.22	0.982
207.85	69.28	2.58	1000	57.74	50	132.42	6.62	0.965
207.85	69.28	2.58	1000	57.74	200	37.77	7.55	0.958
207.85	69.28	2.58	1000	57.74	300	25.41	7.62	0.969
207.85	69.28	2.58	1000	57.74	400	19.14	7.66	0.974
207.85	69.28	2.58	1000	57.74	500	15.37	7.69	0.979
207.85	69.28	2.58	1000	57.74	600	12.85	7.71	0.982
207.85	69.28	2.58	1000	57.74	700	11.05	7.73	0.985
207.85	69.28	2.58	1000	57.74	800	9.69	7.75	0.988

Appendix 5: Comparison of Finite Element Analysis and Theoretical Equation for CFEST Members under Eccentric Compression around Short Axis

$2a$ (mm)	$2b$ (mm)	t (mm)	L (mm)	λ	e_0 (mm)	N (kN)	M (kN×m)	Interaction equation
131.45	109.54	2.99	1200	36.51	5	585.14	2.93	0.975
131.45	109.54	2.99	1200	36.51	20	443.82	8.88	0.997
131.45	109.54	2.99	1200	36.51	40	327.63	13.11	0.985
131.45	109.54	2.99	1200	36.51	60	252.69	15.16	0.951
131.45	109.54	2.99	1200	36.51	80	202.93	16.23	0.916
131.45	109.54	2.99	1200	36.51	100	168.09	16.81	0.885
131.45	109.54	2.99	1200	36.51	300	60.32	18.10	0.974
131.45	109.54	2.99	1200	36.51	500	36.67	18.33	0.991
131.45	109.54	2.99	1200	36.51	800	23.17	18.53	1.003
141.99	101.42	2.96	1200	33.81	5	592.22	3.86	1.021
141.99	101.42	2.96	1200	33.81	20	461.12	12.02	1.044
141.99	101.42	2.96	1200	33.81	40	348.06	18.14	1.037
141.99	101.42	2.96	1200	33.81	60	270.80	21.17	0.998

141.99	101.42	2.96	1200	33.81	80	217.95	22.72	0.957
141.99	101.42	2.96	1200	33.81	500	39.41	25.68	0.997
141.99	101.42	2.96	1200	33.81	800	24.86	25.91	1.008
151.79	94.87	2.91	1200	31.62	5	593.99	2.42	0.987
151.79	94.87	2.91	1200	31.62	20	470.49	7.67	1.021
151.79	94.87	2.91	1200	31.62	40	361.87	11.79	1.027
151.79	94.87	2.91	1200	31.62	60	285.87	13.98	1.001
151.79	94.87	2.91	1200	31.62	80	231.97	15.12	0.966
151.79	94.87	2.91	1200	31.62	300	69.53	17.00	0.987
151.79	94.87	2.91	1200	31.62	500	42.13	17.16	1.001
151.79	94.87	2.91	1200	31.62	800	26.56	17.31	1.012
161.00	89.44	2.87	1200	29.81	5	590.54	2.95	0.984
161.00	89.44	2.87	1200	29.81	20	472.05	9.44	1.015
161.00	89.44	2.87	1200	29.81	40	368.56	14.74	1.028
161.00	89.44	2.87	1200	29.81	100	202.05	20.20	0.947
161.00	89.44	2.87	1200	29.81	300	73.06	21.92	0.989
161.00	89.44	2.87	1200	29.81	500	44.24	22.12	1.003
161.00	89.44	2.87	1200	29.81	800	27.85	22.28	1.013
169.71	84.85	2.82	1200	28.28	5	589.02	2.95	1.011
169.71	84.85	2.82	1200	28.28	20	474.82	9.50	1.036
169.71	84.85	2.82	1200	28.28	40	375.13	15.01	1.049
169.71	84.85	2.82	1200	28.28	60	302.11	18.13	1.029
169.71	84.85	2.82	1200	28.28	80	249.31	19.94	1.001
169.71	84.85	2.82	1200	28.28	100	209.88	20.99	0.970
169.71	84.85	2.82	1200	28.28	300	76.57	22.97	0.995
169.71	84.85	2.82	1200	28.28	800	29.17	23.34	1.020
177.99	80.90	2.77	1200	26.97	40	379.04	13.94	1.026
177.99	80.90	2.77	1200	26.97	60	307.78	16.98	1.012
177.99	80.90	2.77	1200	26.97	80	255.06	18.77	0.987
177.99	80.90	2.77	1200	26.97	100	215.63	19.83	0.960
177.99	80.90	2.77	1200	26.97	300	79.41	21.91	0.987
177.99	80.90	2.77	1200	26.97	500	48.10	22.12	1.002
177.99	80.90	2.77	1200	26.97	700	34.51	22.21	1.008
177.99	80.90	2.77	1200	26.97	800	30.24	22.25	1.011
185.90	77.46	2.72	1200	25.82	5	586.42	2.93	1.018
185.90	77.46	2.72	1200	25.82	60	314.95	18.90	1.035
185.90	77.46	2.72	1200	25.82	80	262.34	20.99	1.009
185.90	77.46	2.72	1200	25.82	100	222.74	22.27	0.981
185.90	77.46	2.72	1200	25.82	500	50.06	25.03	1.001
193.49	74.42	2.67	1200	24.81	40	388.17	15.53	1.033
193.49	74.42	2.67	1200	24.81	60	320.32	19.22	1.026
193.49	74.42	2.67	1200	24.81	80	267.92	21.43	1.003
193.49	74.42	2.67	1200	24.81	100	228.16	22.82	0.978
193.49	74.42	2.67	1200	24.81	300	85.37	25.61	0.984
193.49	74.42	2.67	1200	24.81	500	51.74	25.87	1.001
193.49	74.42	2.67	1200	24.81	800	32.53	26.02	1.010
200.80	71.71	2.63	1200	23.90	5	585.58	2.84	0.997
200.80	71.71	2.63	1200	23.90	20	483.37	9.39	1.016
200.80	71.71	2.63	1200	23.90	80	272.66	21.19	1.004

200.80	71.71	2.63	1200	23.90	100	232.85	22.62	0.980
200.80	71.71	2.63	1200	23.90	300	87.74	25.57	0.982
200.80	71.71	2.63	1200	23.90	800	33.43	25.99	1.009
207.85	69.28	2.58	1200	23.09	5	586.52	2.93	1.013
207.85	69.28	2.58	1200	23.09	20	486.68	9.73	1.028
207.85	69.28	2.58	1200	23.09	80	278.69	22.30	1.014
207.85	69.28	2.58	1200	23.09	100	238.93	23.89	0.991
207.85	69.28	2.58	1200	23.09	300	90.78	27.23	0.980
207.85	69.28	2.58	1200	23.09	800	34.60	27.68	1.008